Continental J. Applied Sciences
El-Jummah *et al*. (2019) 14 (2): 50-67 DOI: 10.5281/zenodo.3376640

Research Article

Flat Wall Cooling Aerodynamics and the Effects of Cross-flow in the Impingement Gap with Single Sided Air Jet Exit Flow using CHT CFD Predictions

[1]El-Jummah A.M*., [2]Andrews G.E., and [2]Staggs J.E.J.
[1]Department of Mechanical Engineering, University of Maiduguri, Nigeria
[2]Centre for Integrated Energy Research, University of Leeds, United Kingdom
***Corresponding Author: al-jummah@hotmail.com**

Abstract

Flat wall impingement cooling investigation was carried out using combined numerical analyses of conjugate heat transfer (CHT) and computational fluid dynamics (CFD) techniques. The analyses were undertaken in impingement array of jet holes with self-induced cross-flow in the impingement gap using a single sided flow exit geometrical model. The aim is to understand the aerodynamics interaction that results to the deterioration of heat transfer with axial distance, as the addition of duct flow heat transfer would be expected to lead to an increase in heat transfer with axial distance. A square array of impingement jet holes was used for a common geometry investigated experimentally, pitch to diameter ratio X/D of 5.0 and impingement gap to diameter ratio Z/D of 3.3 for 11 rows of holes in the cross-flow direction. A metal duct wall was used as the impingement surface with a 100 kW/m^2 imposed heat flux. For a gas turbine combustor cooling application operating at steady state with a temperature difference of ~ 450 K, this heat flux corresponds to a convective heat transfer coefficient (HTC) of ~ 200 W/m^{2}K. A key feature of the predicted aerodynamics was recirculation in the plane of the impingement jets normal to the cross-flow, which produced heating of the impingement jet wall. This reverse flow jet was deflected by the cross-flow, which had its peak velocity in the plane between the high velocity impingement jets. The cross-flow interaction with the impingement jets reduced the interaction between the jets on the surface, with lower surface turbulence (TKE) as a result and this reduced the surface HTC. A significant feature of the predictions was the interaction of the cross-flow with the impingement jet wall and associated heat transfer to that wall. The results showed that the deterioration in heat transfer with axial distance was well predicted together with predictions of the impingement gap exit pressure loss.

Keywords: Investigation, analysis, techniques, interaction, geometry, array

Received: 21 Dec 2018 Accepted: 12 Feb 2019

ISSN: 1597 – 9928. Science and Education Development Inst., Nigeria

Introduction

Improved cooling of gas turbine (GT) combustor and turbine blade walls for effective power generation, critically depends on the advances in the GT thermal efficiency that obviously rely on the turbine entry (or combustor exit) temperature. This is because, the GT combustion temperature that influences the efficiency are well in excess of the melting point of the component metal walls material (Brooks, 2010, Isiako *et al*. 2009). The combined use of effective cooling techniques with sufficient thermal resistance materials is the reason why the high operational temperature of the GT components can be achieved. Impingement air jet cooling that has been shown, to be the most effective cooling methods of GT component walls (Karcher and Tabakoff, 1970, Kumada and Mabuchi, 1970, Chance, 1974, Andrews and Hussain, 1984, Facchini and Surace, 2006, Andrews *et al*. 2011, El-jummah *et al*. 2013a, b), enables the cooling air used to be minimized. For turbine blades, it improves the cycle thermal efficiency and lowers carbon dioxide (CO_2) emissions (El-jummah *et al*. 2014a, b, 2016, 2017, 2018, 2019). The impingement geometry investigated here is typical of a low NOx primary zone combustion chamber wall (Abdul Hussain and Andrews, 1990), where the impingement efflux is discharged as the main combustion air as Figure 1a shows. Impingement cooling is also used for cooling combustor transition duct or for the primary low the NOx region only and then the impingement air is passed into combustor as film cooling or as part of the dilution air. This method of primary zone cooling is used in several industrial gas turbines.

The geometrical setup shown in Figure 1b in terms of X/D and Z/D, is also similar to those used in turbine blade cooling and was investigated experimentally by Florschuetz *et al*. (1981), El-jummah *et al*. (2013a, 2014a, b). Horlock *et al.* (2001) had shown that film cooling of turbine blades results in the deterioration of the turbine efficiency and that the maximization of impingement cooling enables the film cooling mass flow to be minimized and hence has an impact on the cycle efficiency. Chance (1974), El-jummah *et al*. (2014a) showed that a significant problem with impingement cooling was that the outflow of air in one direction led to a deterioration in the wall heat transfer. This is a problem in cooling design, particularly for combustor walls where the distances to be cooled are greater than in turbine blades. However, the reasons for this deterioration in heat transfer are not well understood and are often simply ascribed to the deflection of the impingement jet by the cross-flow. Experimental results (Chance, 1974) and CFD predictions (El-jummah *et al*. 2013a, 2014a) showed that for high X/D with very high air jet velocities and relatively low impingement gap cross-flow velocities, this deterioration of heat transfer with axial distance still occurred. As the flow in a duct has a significant heat transfer on its own (Andrews *et al*. 2007) and if the impingement and duct flow heat transfer were additive,

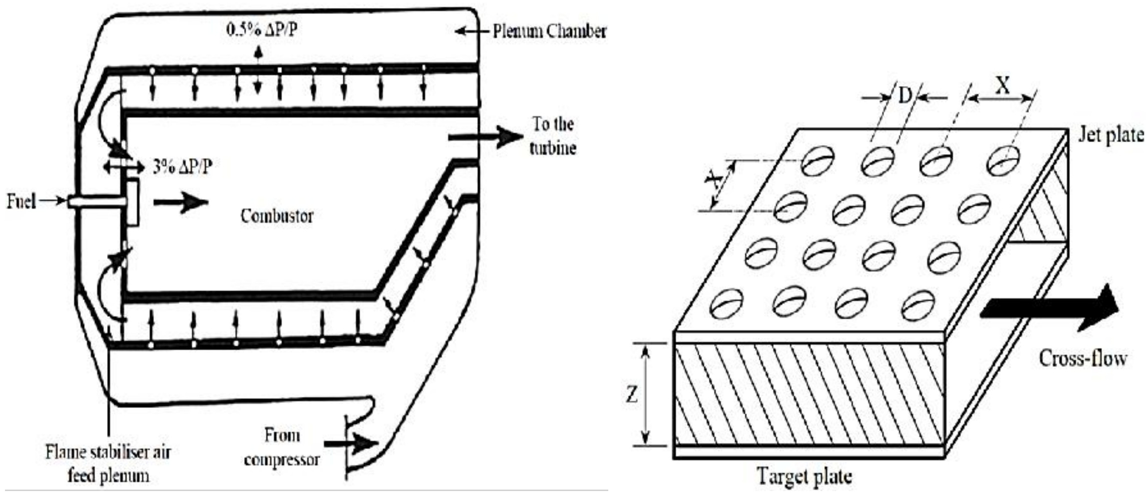

(a) Gas turbine combustor (b) Flat wall geometrical setup

Figure 1: Gas turbine regenerative cooling combustor with single exit jet flow

then the heat transfer would increase in the downstream direction. This does not occur in any experiments on impingement cooling with single sided exit, but in the CFD prediction of El-jummah *et al*. (2013a, 2014a, b).

The purpose of this present work is to use CFD to understand the complex flows in the impingement duct and the interactions with the outflow from the upstream impingement holes by the downstream impingement jets. In practical applications of combustor wall cooling, the lengths that must be cooled necessitate a large number of holes and by increasing the number of holes adds to the computational overhead in CFD (El-jummah *et al*. 2014b. This present work investigated the modelled grid geometry of 11 rows of impingement cooling square array of holes for an X/D of 5, Z/D of 3.3 and L/D of 2.12. Experiments on the influence of cross-flow on impingement heat transfer have used both a single row (Metzger and Korstad, 1970) and multi-jet arrays (Andrews *et al*. 1985) of holes. Most investigators found that cross-flow reduced the impingement heat transfer, even though the impingement jet velocity was high and the jet deflection by the cross-flow was small (Andrews and Hussain, 1987).

Review of Experimental Investigation on Impingement Gap Cross-flow

Florschuetz *et al.* (1981) found for a 10 row impingement array of holes that the trailing edge heat transfer was between 20 and 41 % below that of the leading edge for a range of geometries, most of which had flow mal-distribution. Kercher and Tabakoff (1970) found the trailing edge heat transfer was lower than the leading edge heat transfer by between 5 and 41 %, which also depended on the geometry. The greatest effect was for N of 12, X/D of 6.3 and Z/D of 3.9, for which is similar to the geometry investigated in the present work. Abdul Hussain and Andrews (1990) investigated using the experimental rig shown in Figure 2, the impingement heat transfer with a single sided exit and no initial cross-flow, for 10 row of jet hole geometry similar to the one modelled in the present work. The flow separation, reattachment and development, as in Figure 2a (Cho and Goldstein, 1986) that was caused by the influence of vena contracta (El-jummah *et al*. (2013b, c) could also impact on cross-flow due to the increased velocity. Also shown to be significant to cross-flow effects is the experimental short hole in Figure 2b (Treumen *et al*. 1994), even though the hole internal rough surface could affect the pressure loss. These experimental concerns have been verified using CFD predictions by El-jummah et al. (2013a, 2014a, 2015), to be the major problem of flow mal-distribution that occurs due to the cross-flow with pressure loss being significant relative to the impingement wall static pressure.

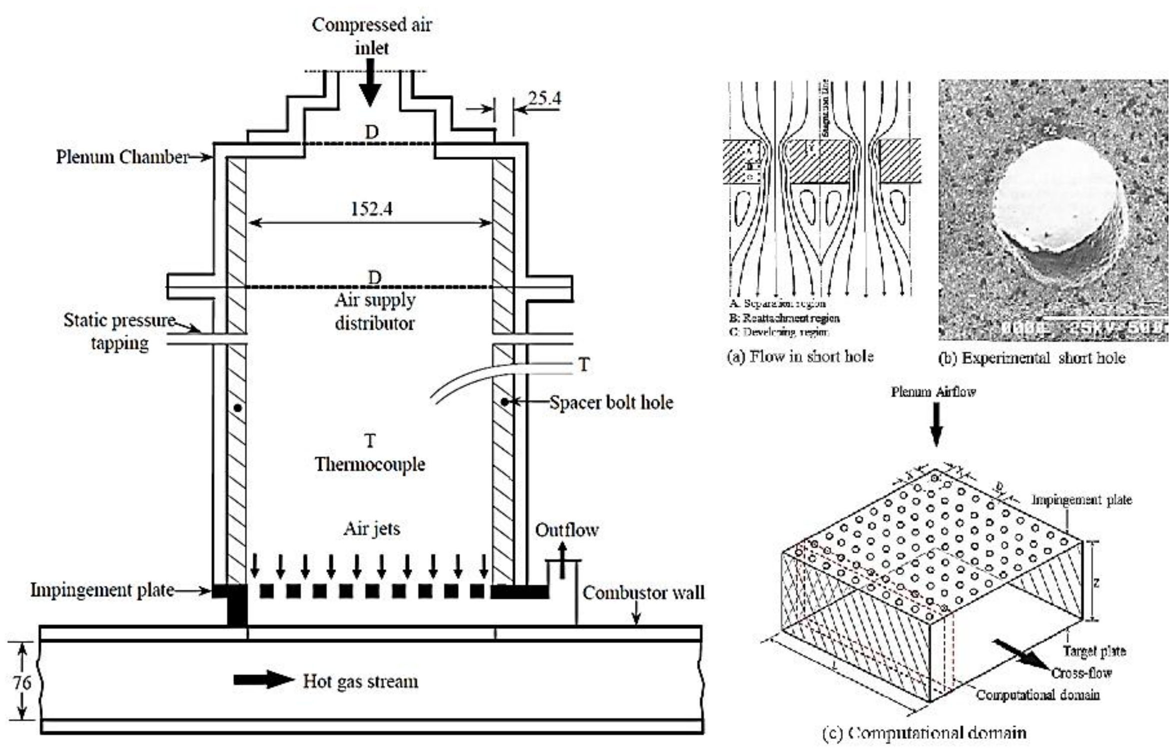

Figure 2: Experimental rig and setup of the impingement jet cooling on the target wall

Review of Computational Investigation on Impingement Gap Cross-flow

Previous CFD investigations of impingement cooling have not been primarily directed at the cross-flow effect and have not used a large number of upstream holes, apart from a previous attempt using much coarser grid of this configuration by Andrews *et al.* (2007). The complex recirculation in the impingement gap and the interaction between adjacent jets on the target surface presents a challenge for CFD predictions (El-jummah *et al*. (2015a, b). The flow distribution and the heat transfer coefficients *h*, on the liner of gas turbine combustor for jets impingement and cross-flow were predicted by Bailey *et al.* (2003). The use of steady state isothermal conditions that were employed experimentally (Andrews and Hussain, 1984, Andrews *et al*. 1985) was also applied for the CFD impingement analysis (Andrews *et al*, 2011, Wang *et al*. 2011). Recently, El-jummah *et al*. (2018, 2019) predicted the influence of impingement gap cross-flow on thermal gradients using high mass flow rate and with obstacles in the gap. Often, impingement cooling CFD investigators uses the RANS turbulent models, especially the two equation model (Bailey *et al.*, 2003, Taslim and Rosso, 2012), because the turbulence is considered to be isotropic in the complex stirred flow in the impingement gap. CFD simulation enables the prediction of the flow fields that characterizes air jet impingement cooling (Sharif and Mothe, 2010), which also reveals the conjugate heat transfer (CHT) characteristics (El-jummah *et al*., 2014). Both structured (Wang *et al*. 2011, El-jummah *et al*. 2014a) and unstructured (Sharif and Mothe, 2010) or hybrid (Anand and Jubran, 2011) grids have been used, which normally depended on the complexity of the geometry. The present work uses CHT CFD analysis that also visualizes the heated coolant flow reflected from the hot target surface using dimensionless temperature. Cooling air was at ambient temperatures ~ 300 K, with inlet velocity that determined the hole Reynolds number, Re (El-jummah *et al*. 2014a, b) and the grid geometry was modelled using the computational domain or setup (El-jummah *et al*. 2019) shown in Figure 2c.

CFD Methodology

Computational Grid Model

Table 1 is the list of variables and dimensions that were used in modelling the impingement grid geometry shown in Figure 3, which was modelled using the symmetrical schematic approach shown in Figure 2c. The impingement geometry was a square array of holes with an X/D of 5.0 and 11 rows of air holes. An additional row of holes was added to the model compared with the experiments to avoid any passage end effects in the computational analysis. The specific geometry modelled in the present work is given in Table 1 and it has an impingement jet air hole wall thickness of

ISSN: 1597 – 9928. Science and Education Development Inst., Nigeria

6.35 mm and is typical of that used in some large industrial gas turbine combustors. The three dimensional model was discretized using a structured grid in ANSYS ICEM meshing tool with cell concentration higher at the impingement and target walls. The test walls are represented by cells of the same cross sectional area that are rectangular but quadrilateral around the air hole surfaces as in Figure 3. El-jummah *et al*., (2013c, 2014a) reported the results for grid independence in the range of grid cells of 10^5 to ~ 1.5×10^6 and based on Table 2 boundary conditions, which were computed using the standard k - ε turbulence model with y^+ value ~ 35. A representative Nusselt number at the target wall was computed to investigate the influence of the number of computational cells on heat transfer. Figure 4 is the results which indicated that at least 10^6 cells are adequate to reduce any effect of grid sensitivity. The chosen grid that was shown to adequately resolve any influence of the cross-flow on the velocity profile of the impingement jet discharge and also compute the flow separation at the air hole inlet is 1.3×10^6. Hence, with ~1120 nodes (~ 60 nodes per plane) in each air hole, the number of cells could also not be too large for a normal HPC system, which this CFD investigation is also applying.

The geometry modelled was also similar to the experimental test facility used by Abdul Husain and Andrews, (1990) as Figure 2 show. It consists of an internal cross-sectional area of 152 mm square test section with a plenum chamber that was lagged with 25 mm thick thermal insulation, which is considered as a boundary condition with no heat flux in the computation. Compressed air at ambient temperature of ~ 300 K flows through the plenum inlet from the supply (Abdul Husain *et al*., 1988), which then flows through the holes array, to cool the metal target wall below the jet wall. The hot gas flow in the

Table 1: Impingement jet cooling geometrical parameters

Variables	Dimensions
D (mm)	3.00
X (mm)	15.00
Z (mm)	10.00
L (mm)	6.35
L/D	2.12
X/D	5.00
Z/D	3.30
X/Z	1.50
A	3.14 %
n	4444 m^{-2}
Array	11 × 11

ISSN: 1597 – 9928. Science and Education Development Inst., Nigeria

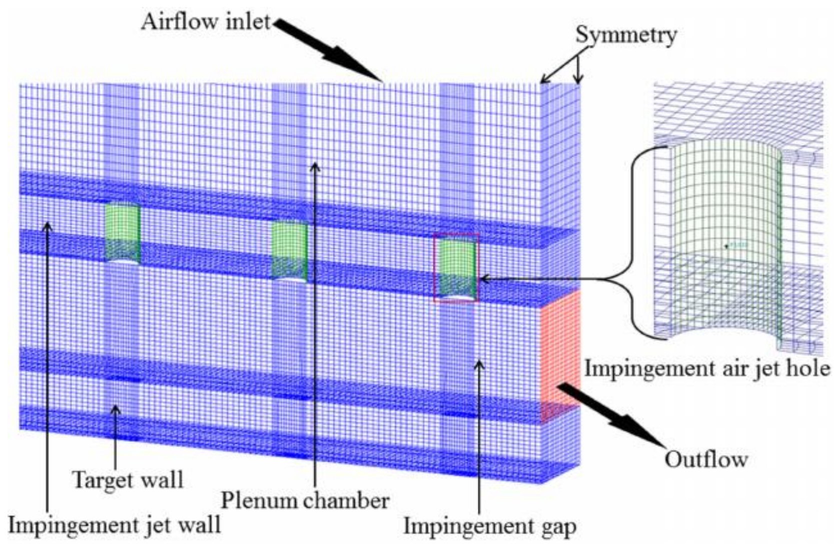

Figure 3: The impingement jet cooling heat transfer computational grid geometry

Table 2: Computational flow boundary conditions

G (kg/sm²bar)	**1.90**
V_{in} (m/s)	1.60
V_j (m/s)	43.41
U_c (m/s)	24.0
V_j/U_c	1.8
Re_h $(=\rho V_j D/\mu)$	9200
T_∞ (K)	298
q'' (W/m²)	100
ρ (kg/m³)	1.178

duct below the target wall was not modelled explicitly, but instead a constant heat flux of 100 kW/m² was applied as the boundary condition along the target wall. This heat flux approximately reproduces the conditions of the hot rig of Abdul Husain *et al*., (1990), with a coolant to hot gas temperature difference of ~ 450 °C and convective heat transfer coefficient (HTC), *h* at the cooled surface of ~ 200 W/m² K. Figure 5 shows the significance of using lower β to achieve optimum jet cooling heat transfer (El-jummah, 2015) that was expected to resolve any effect of wall thermal gradient, an important component that indicates adequate and uniform cooling. Figure 5 shows that cooling heat transfer is proportional to β, an indication that cooling critically depends on mass flux, geometry and grid refinement (Sharif and Mothe, 2010, El-jummah *et al*. 2015a, b).

ISSN: 1597 – 9928. Science and Education Development Inst., Nigeria

Computational Procedures

The numerical calculations of the present CHT CFD work were carried out based on the boundary conditions (El-jummah *et al*., 2013a) shown in Table 2 and with the grid modelled geometry shown in Figure 3. The computational procedure is the same as that previously validated (El-jummah *et al*. 2014a, b, 2016, 2017, 2018, 2019). The standard k - ε turbulence model in ANSYS Fluent was used with a wall function y^+ value of ~ 35, this y^+ value was in the range of the near wall law of the wall of $30 < y^+ < 300$. The use of the k - ε model was because the flow aerodynamics in the impingement gap are major aspects of the flow that are characterized with strong flow recirculation and the impingement jet holes characterized with flow reattachment and separation (Cho and Goldstein, 1986, El-jummah *et al*. 2015b), hence it has good prediction capabilities, as also shown by Figure 4. The convergence criteria were set at 10^{-5} for continuity, 10^{-11} for energy and 10^{-6} for k, ε and momentum (x, y and z velocities), respectively. These were selected in order to ascertain that the likely errors are within the limit of acceptability and hence the predicted data also, are expected to certify the experimentally sorted data by Abdul Hussain and Andrews, 1990. Equations 1 and 2 were used to predict the data of Figures 4 and 5, respectively, for which the experimentally acceptable error depends on whereby 5 is used to predict the HTC data.

$$Nu = \frac{hD}{k_f} \tag{1}$$

$$h = \frac{q''}{\left(T_s - T_\infty\right)} \tag{2}$$

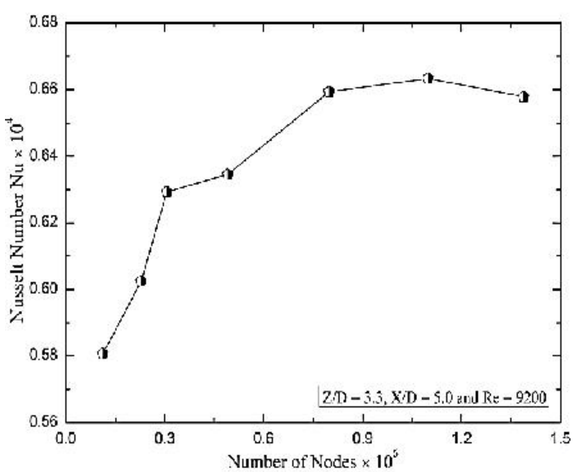

Figure 4: Grid independence test for range of cells modelled (El-jummah *et al*. 2014a)

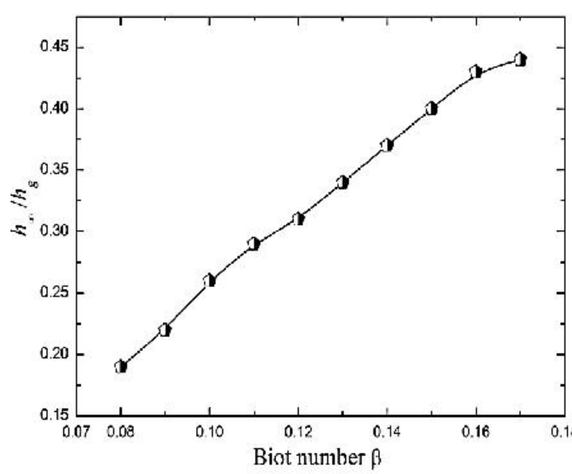

Figure 5: Influence of cooling effectiveness on Biot number with impingement jet flow

ISSN: 1597 – 9928. Science and Education Development Inst., Nigeria

Results and Discussion

The Predicted Velocity Profiles in the Impingement Holes and Duct

The predicted flow pattern for the two upstream and downstream holes is represented in contour plots for the velocity and is shown in Figure 6a and b. It shows the magnitude of the air jet velocity in each of the hole shown and in the impingement gap for the plane on the centre-line of the impingement row of jets. It is in this plane that the cross-flow velocity is at a maximum, so the velocities are low at the leading two holes and increase at the last two holes. Figure 6c and d shows the velocity profile in the plane at 90^{o} to those in Figure 6a and b, which are for the plane on the centre-line of the holes and is shown for the second and last hole. Here, it shows that the cross-flow passes between the jets and this is a low velocity at the second hole, as there is only one upstream hole, but it increases significantly at the last hole. At the last hole the coolant jet is deflected away from being in-line with the hole and hits the target surface further downstream, as shown in Figure 6d. Both indicates that the highest velocity is in the centre of the hole and this is the influence of the vena contracta, as was explained above for Figure 2a.

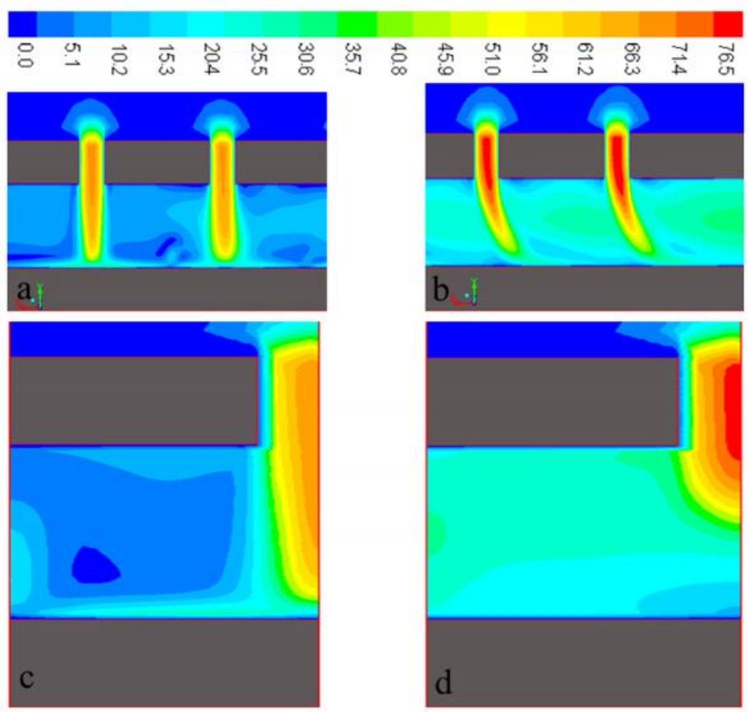

Figure 6: Predicted contour of velocity magnitude (m/s) in the impingement gap

ISSN: 1597 – 9928. Science and Education Development Inst., Nigeria

Figure 7a and b shows the predicted pathlines velocity of the leading hole and the exit hole, it shows the influence of reverse jet in the leading hole area, which was anticipated to affect the impingement jet wall by heating it. It flows in the opposite direction to the impingement jets and on the centre point between a four-hole array of impingement jets, as Figure 7a shows. After the fourth row of holes the cross-flow normally dominates (El-jummah et al. 2013a), which impacts on the reverse jets by blowing it away towards the exit, as shown in Figure 7b. This is the obvious reason why, the air velocity in the downstream holes is ~ 20 % higher than that in the upstream holes, as in Figure 8a and b and is expected to also affect the exit hole pressure loss.

The Predicted Flow Mal-distribution in the Jet Holes

The velocity contours on the centre line of the first and last jet holes were shown in Figure 6c and d, respectively, it shows that the flow at the jet hole outlets is not uniform with the axial distance. This was verified by the outlet jet velocity profiles in Figure 8, eventhough none of the profiles are fully developed turbulent

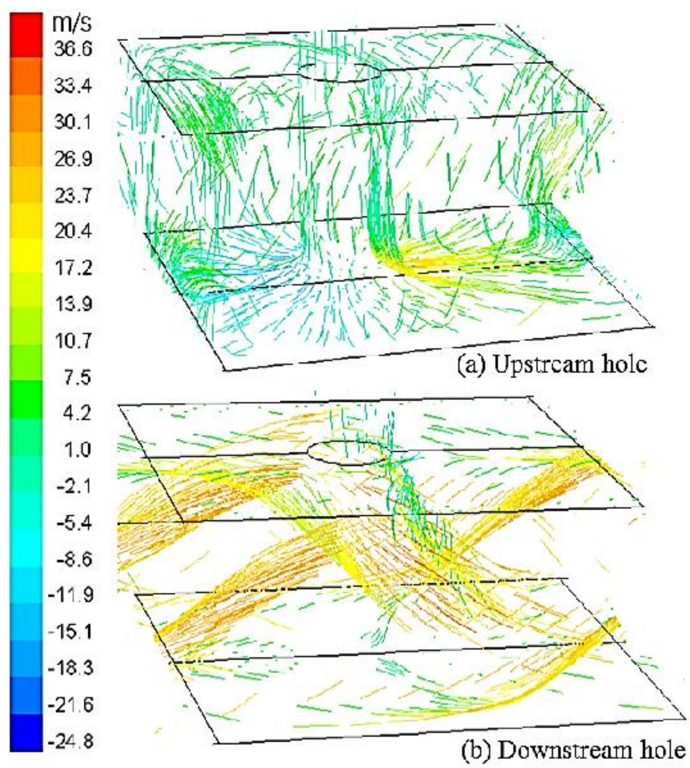

Figure 7: The predicted impingement gap velocity pathlines (m/s)

flow and at the leading hole, the profile is symmetric and closer to parabolic than the flatter turbulent pipe flow velocity profiles. This is because of the sharp edged entry to the impingement air hole from the plenum chamber and the flow separation in the jet hole inlet due that was caused by the impact of vena contracta. Also followed due the effects shown, is the flow reattachment to the jet walls about half way long the short holes, hence insufficient distance to achieve fully developed pipe flow turbulence. At the last hole, the presence of impingement gap cross-flow acts to skew the velocity profile at the hole outlet in the downstream direction. This is anticipated to result in distorting the turbulence and impingement heat transfer in the downstream direction of the target wall.

The 3D particle paths velocity of Figure 7 clearly showed the reverse jet flowing between the impingement jets of the first two rows of holes. The reverse flow jet deflects toward the exit plane and this trend increases along the gap to the exit plane. Figure 7 also shows that this centre-line reverse flow jet is deflected by 45^{o} and is intensified by the gap cross-flow. This jet has a strong impingement on the wall well downstream of the holes that started the interaction as in Figure 7. However, this impingement is at a lower velocity then at the leading edge and the distribution of turbulence around the jet is adverted downstream, as will be shown below. The predicted impingement air jets velocity enables the mean velocity of each hole to be determined. This velocity was calculated in the middle of the hole, to avoid any inlet and outlet flow recirculation zones. The mean velocity for each hole is shown in Figure 9, normalized to the mean (or jet) velocity, V_j for all the holes, which is set by the total mass flow of coolant for which the computation was carried out, as detailed in Table 2. Figure 9 shows that for the present geometry investigated, a flow mal-distribution with the leading holes receiving 7 % less air and the last holes receiving 9 % more air exists. This strongly supports the view that the flow mal-distribution is driven by the static pressure difference along the impingement duct, as depicted by work of El-jummah *et al*. (2013b and c). Also in Figure 9 is the comparison of the flow mal-distribution of the present prediction with the work of El-jummah *et al*. (2014a and 2019), which all were shown to be in the same trend. But the present work prediction indicates much higher mal-distribution, which possibly was because of the addition of extra one hole to represent the plenum end effects. Also, the predictions by El-jummah *et al*. (2019) was about ~ 10 % lower than this prediction, because of the presence of obstacles on the target wall there that distracts the impingement gap cross-flow, which also affects the hole flow mal-distribution.

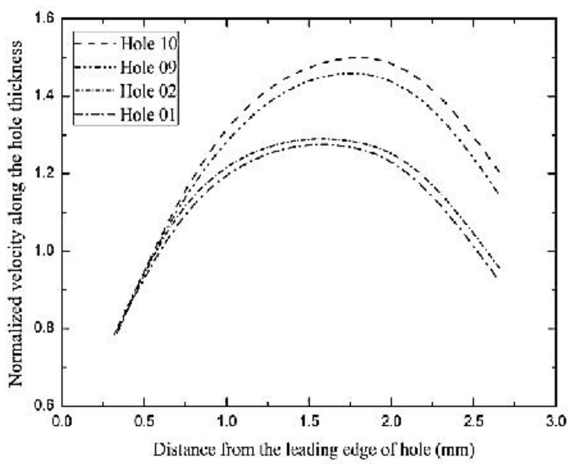

Figure 8: The impingement air jet velocity profile for two up and down-streams holes

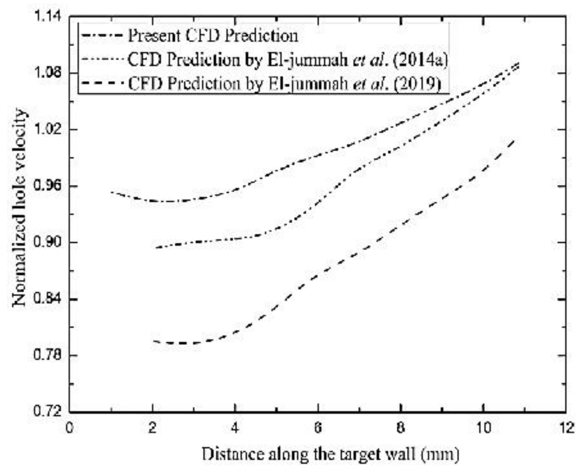

Figure 9: Comparison of the jet hole flow mal-distribution of the impingement jets

Prediction of the Pressure Loss along the Impingement Gap

The predicted static pressure loss across the impingement wall as a function of axial distance is shown in Figure 10 and was compared with the measured data of El-jummah *et al*. (2014a). This was determined as the pressure difference between the air supply from the plenum and the static pressure on the impingement gap side of the impingement wall at the centre of the four jet holes. Figure 10 clearly shows that the lower flow through the leading holes gave a lower pressure loss and the comparison shows good agreement with the experimental data. The difference in static pressure between the first air hole pressure loss and the last is the pressure loss of the cross-flow down the gap and added 0.45 % pressure loss to that across the first hole. This cross-flow velocity pressure loss is the source of energy for the generation of turbulence by the cross-flow, as it interacts with the impingement jets. The predicted overall pressure loss of 2.45 % is really in good agreement with the measured pressure loss of 2.4 % at this flow condition. This indicates that the flow aerodynamics in the jet holes and the impingement gap are correct, as these are the major determining factor that influences the pressure loss.

The Predicted Axial Variation of the Surface Average Heat Transfer Coefficient

The predicted heat transfer coefficient (HTC), h was surface averaged for each impingement hole, which cooled a surface area of X^2 within the impingement jet directed at the centre of the target wall. The axial variation of the HTC averages are shown in Figure 11 and was compared with the experimental data of AbdulHusain and

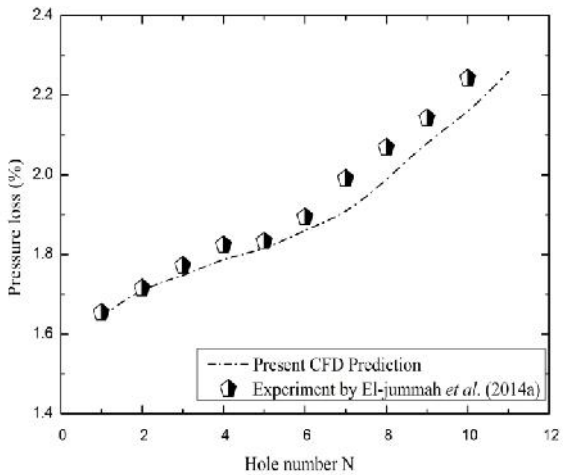

Figure 10: Comparison of predicted pressure loss along the impingement gap exit holes

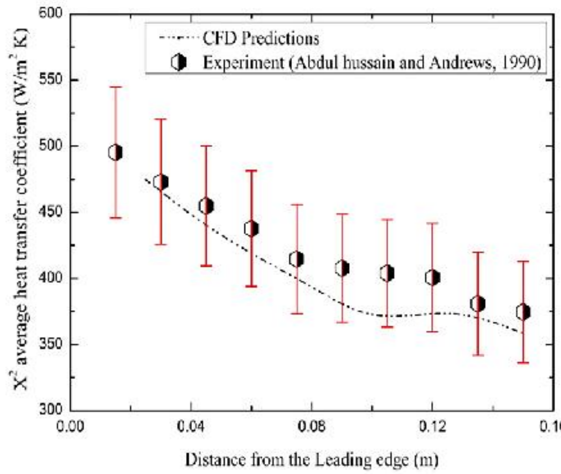

Figure 11: Comparison of the axial distance X^2 average HTC in the cross-flow direction

Andrews, (1990) with a ± 10 % error. The numerical agreement in Figure 11 with the measured surface average X^2 HTC values was very good at the leading edge for the nimonic - 75 wall. The agreement for the first five and the last two impingment jets was perfectly good, then overprediction at hole 6, 7 and 8, which is the same outcome to that predicted for the pressure loss. The disagreement over 6 - 8 holes of the impingement gap is a maximum of 6 % high at hole 7 for the CFD compared with the experiments and this is within the error bar, hence the prediction is within the acceptable range.

Prediction of the Locally Surface Average Normalized Temperature

Figure 12 shows the locally X^2 average normalized temperature over the target surface along the axial distance of the impingement gap. The increased in normalized temperature along the axial distance clearly explained why the X^2 average HTC decreases with distance from the leading edge. This result indicates that the higher the HTC with turbulence, the lower will be the wall surface normalized temperature and the better is the surface cooling. Therefore, any decrease in surface or locally X^2 average HTC, is also expected to results into an increased wall thermal gradient across the wall thickness (El-jummah *et al*. 2013c, 2018, 2019). Also, this could affect the cooling with a reverse flow by impingement air jet on the jets plate, which could also result into heating of the jets plate (El-jummah *et al*., 2013a, 2014a) and has been shown to influence the cooling of the target walls.

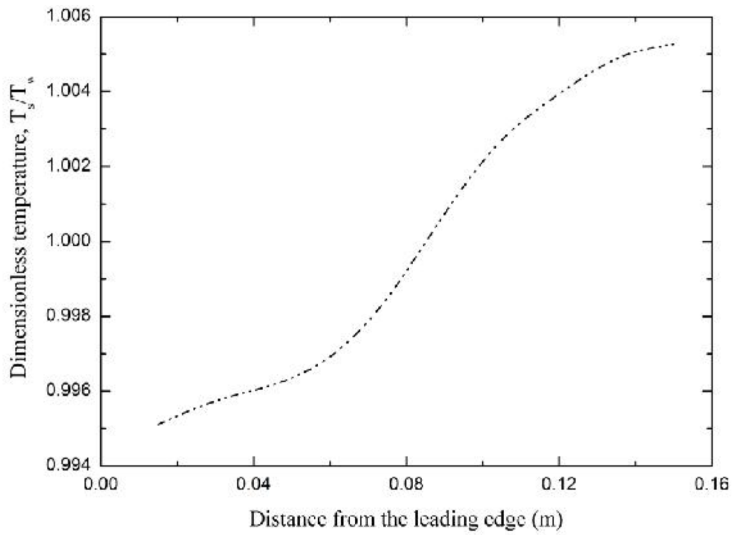

Figure 12: The predicted X^2 average normalized temperature in the cross-flow direction

Conclusions

The CFD results showed that the impact of the cross-flow was to strongly deflect the reversed flow jets on the centre of each of four impingement jet holes. The reversed jets were deflected at 45^o by the 10^{th} impingement jet hole position, this impacts on the cross-flow velocity that affects the turbulence levels on the impingement wall, which reduces the heat transfer coefficients. This concludes that CFD could optimise the design of impingement cooling system of gas turbines, in order to predict and analyse the complex characteristics of the systems.

The complexity of the aerodynamics of impingement flow with large number of holes and flow exit in one direction has been clearly demonstrated. The importance of the reverse impingement flow on the impingement jet surface has been emphasised and the role of the cross-flow in interacting with this reverse flow jet has been demonstrated.

The predicted X^2 surface average axial variation of the heat transfer coefficent was well predicted, especially over the first 5 rows of holes. The agreement was good and it falls within the measured error bar.

The predicted wall temperature profiles showed much lower temperature gradients than gradients in the surface heat transfer. This illustrates the action of internal wall conduction in smoothing out the large convective heat transfer gradients. The largest thermal gradients were predicted to be through the thickness of the wall at 6.3 k/mm.

ISSN: 1597 – 9928. Science and Education Development Inst., Nigeria

Conjugate heat transfer CFD work that was undertaken is to try to elucidate the aerodynamic interactions that result in the deterioration of target wall heat transfer with axial distance of the impingement cooling system with a single sided flow exit. The square array of the impingement jet holes, where flow mal-distribution between the rows of impingement jet holes that was predicted to be small, indicates that the grid model is a good geometry for the CFD analysis.

Nomenclature

A	Impingement hole porosity $((\pi/4)\,D^2)/X^2$
D	Impingement air hole diameter, m
G	Coolant Mass flux, kg/sm²bar
h	Heat transfer coefficient (HTC), W/m²K
k_f	Thermal conductivity of fluid, W/m K
L	Test wall metal thickness, m
n	Number of jet/unit surface area, m^{-2}
N	Number of upstream rows of imp. holes
Nu	Nusselt Number
ρ	Density of air, kg/m³
ΔP	Impingement wall pressure loss, Pa
P	Coolant supply static press. (app. 1 bar)
Pr	Prandtl number
Re	Reynolds number
T_∞	Coolant temperature, 288 K
T_S	Target surface metal wall temp., K
T_w	Target wall imposed temp. (360 K)
V_j	Impingement jet mean velocity, m/s
v	Kinematic viscosity, m²/s
X	Hole to hole pitch, m
Z	Plate to plate gap, m
ξ	Grid cell size, m

Subscripts

C	cross-flow
j	Jet
s	Surface
f	fluid
∞	Coolant

References

Abdul Husain R. A. A. and Andrews G. E. (1990). "Full Coverage Impingement Heat Transfer at High Temperature," ASME Paper 90-GT-285, pp. 1-12.

Abdul Husain R. A. A., Andrews G. E., Asere A. A. and Ndiema C. K. W. (1988). "Full Coverage Impingement Heat Transfer: Cooling Effectiveness," ASME Int. Gas Turbine Conference, ASME Paper 88-GT-270, pp. 1 - 9.

Anand K. and Jubran B. A. (2011) "Computational Study of Micro-jet Impingement Heat Transfer in a High Pressure Turbine Vane," in Proc. ASME Turbo Expo 2011, ASME Paper GT-45267, pp. 1-12.

Andrews G. E. and Hussain C. I. (1984). "Impingement Cooling of Gas Turbine Components," High Temperature Technology, Vol. 2 (2): 99-106.

Andrews G. E. and Hussain C. I. (1986). "Full Coverage Impingement Heat Transfer: Influence of Channel Height," presented at the Eight Int. Heat Transfer Conference.

Andrews G.E., Wang J. and Abdul Hussain R. A. A. (2011). “CFD Predictions of the Aerodynamics and Heat Transfer from Arrays of Impinging Jets with Cross-flow”. International Gas Turbine Congress 2011, Osaka, IGTC 2011-0141.

Andrews G. E. and Hussain C. I. (1987). "Full Coverage Impingement Heat Transfer: The Influence of Cross-flow," AIAA-87-2010, pp. 1-9.

Andrews G. E. and Khalifa I. M. (2007). "Planar duct heat transfer with turbulence enhancing obstacles for combustor liner external cooling," Proc. ASME IGTI International Gas Turbine Congress: Power for Land, Sea and Air. 2007, Montreal. ASME Paper GT - 27418.

Andrews G. E., Abdul Husain R. A. A. and Mkpadi M. C. (2006). "Enhanced Impingement Heat Transfer: The Influence of Impingement X/D for Interrupted Rib Obstacles (Rectangular Pin Fins)," J. Turbomachinery. Trans. ASME, vol. 128 pp. 321-331.

Andrews G. E., Asere A. A., Hussain C. I. and Mkpadi M. C. (1985). "Full Coverage Impingement Heat Transfer: The Variation in Pitch to Diameter Ratio at Constant Gap," Proportion and Energetics Panel of AGARD, 65th Symposium, 'Heat Transfer and Cooling in Gas Turbines', ASME Paper 26, pp. 1-12.

Andreini A., Da Soghe R., Facchini B., Maiuolo F., Tarchi L. and Coutandin D. (2012). "Experimental and Numerical Analysis of Multiple Impingment Jet Arrays for an Active Clearance Control System".Proc. ASME Turbo Expo 2012, ASME Paper GT2012-68791.

Bailey J. C., Intile J., Fric T. F., Tolpadi A. K., Nirmalan N. V. and Bunker R. S., "Experimental and Numerical Study of Heat Transfer in a Gas Turbine Combustor Liner," J. Eng. Gas Turbines and Power. Transactions of the ASME, vol.125, pp.994-1002, 2003.

Brooks F. J. (2010) "GE Gas Turbine Performance Characteristics," *GE Power Systems,* vol. GER-3567H, pp. 1-16.

Chance J. L. (1974). "Experimental Investigation of Air Impingement Heat Transfer under an Array of Round Jets," *Tappi,* vol. Vol.57, No.6, pp. 108-112.

Eisako I., Ikuo O. and Keizo T. (2009). "Development of Key Technologies for the Next Generation 1700^{o}C-Class Gas Turbine," Proc. ASME Turbo Expo 2009: power for Land, Sea and Air, ASME Paper GT - 59783, pp. 1-11.

El-jummah A. M., Andrews, G. E. and Staggs J. E. J. (2013a). "Conjugate Heat Transfer CFD Predictions of Impingement Jet Array Flat Wall Cooling Aerodynamics with Single Sided Flow Exit". Proc. ASME Turbo Expo Conference, GT-95343**,** 1 - 12.

El-jummah A. M., Andrews G. E. and Staggs J. E. J. (2013b). "Conjugate Heat Transfer

CFD Predictions of the Influence of the Impingement Gap on the Effect of Cross-Flow". Proc. ASME Heat Transfer Conference, HT-17180**,** 1 - 12.

El-jummah A. M., Abdul Hussain R. A. A., Andrews G. E. and Staggs J. E. J. (2013c). "Conjugate Heat Transfer CFD Predictions of the Surface Averaged Impingement Heat Transfer Coefficients for Impingement Cooling with Backside Cross-flow". *Proc. ASME IMECE Conference,* IMECE-63580**,** 1 - 14.

El-jummah A. M., Abdul Hussain R. A. A., Andrews G. E. and Staggs J. E. J. (2014a). "Conjugate Heat Transfer Computational Fluid Dynamic Predictions of Impingement Heat Transfer: The Influence of Hole Pitch to Diameter Ratio X/D at Constant Impingement Gap Z". Trans. ASME J. Turbomachinery, 136 (12), 1 - 16.

El-jummah A. M., Abdul Hussain R. A. A., Andrews G. E. and Staggs J. E. J. (2014b). "Conjugate Heat Transfer CFD Predictions of Impingement Heat Transfer: Influence of the Number of Holes for a Constant Pitch to Diameter Ratio X/D". Proc. ASME Gas Turbine Conf., GT-25268**,** 1 - 14.

El-jummah A. M. (2015). Impingement and Impingement/Effusion Cooling of Gas Turbine Components: Conjugate Heat Transfer Predictions. The White Rose UK: A Ph D Thesis, University of Leeds.

El-jummah A. M., Andrews G. E. and Staggs J. E. J. (2015a). "CHT/CFD Predictions of Impingement Cooling With Four Sided Flow Exit". Proc. ASME Turbo Expo, GT-42256, 1 - 12.

El-jummah A. M., Andrews G. E. and Staggs J. E. J. (2015b). "Conjugate Heat Transfer CFD Predictions of Metal Walls with Arrays of Short Holes as Used in Impingement and Effusion Cooling". Int. Gas Turbine Congress (IGTC), Tokyo.

El-jummah A. M., Andrews G. E. and Staggs J. E. J. (2016). Impingement Jet Cooling with Ribs and Pin Fin Obstacles in Co-flow Configurations: Conjugate Heat Transfer Computational Fluid Dynamic Predictions. Proc. ASME Turbo Expo: Turbomachinery Technical Conference & Exposition, GT- 57021, 1 - 16.

El-jummah A. M., Oluwole F. A., Andrews G. E. and Staggs J. E. J. (2017). Numerical Predictions of Enhanced Impingement Jet Cooling with Ribs and Pins in Co-flow and Cross-flow Configurations. Arid Zone Journal of Engineering, Technology and Environment Vol. 13 (1): 149-162.

El-jummah A. M**.**, Andrews G. E. and Staggs J. E. J. (2018). "Enhancement of Impingement Heat Transfer with the Crossflow Normal to Ribs and Pins Between each Row of Holes". Proc. ASME Turbo Expo: Turbomachinery Technical Conf. & Exposition, GT - 76969, 1 - 13.

ISSN: 1597 – 9928. Science and Education Development Inst., Nigeria

El-jummah A. M., Andrews G. E. and Staggs J. E. J. (2019). "Predictions of Impingement Heat Transfer with Dimples, Pin-fins and Zig-zag rib Obstacles: Conjugate Heat Transfer Computational Fluid Dynamics Predictions". Proc. ASME Turbo Expo: Turbomachinery Technical Conf. and Exposition, GT - 90730, 1 - 12.

Facchini B. and Surace M. (2006). "Impingement Cooling for Modern Combustors: Experimental Analysis of Heat Transfer and Effectiveness," Experiments in Fluids. Springer, Vol. 40, pp. 601 - 611.

Florschuetz L. W., Truman C. R. and Metzger D. E. (1981). "Streamwise Flow and Heat Transfer Distributions for Jet Array Impingement with Cross-flow," Trans. ASME, J. Heat Transfer, Vol. 103, pp. 337-342.

Horlock J. H., Watson D. T. and Jones T. V. (2001). "Limitations on Gas Turbine Performance Imposed by Large Turbine Cooling Flows," J. Eng. for Gas Turbine and Power. Transaction of the *ASME,* Vol. 123, pp. 487-494.

Kercher D. M. and Tabakoff W. (1970). "Heat Transfer by a Square Array of Round Air Jets Impinging Perpendicular to a Flat Surface including Effects of Spent Air," ASME J. Eng. Power, pp. 73-82.

Kumada M. and Mabuchi I. (1970). "Studies on the Heat Transfer of Impinging Jet," 1st Report, Mass Transfer for Two-Dimensional Jet of Air impinging Normally on a Flat Plate, Vol. 13, No. 55, pp. 77-85.

Lee C. S., Shih T. I. P., Bryden, K. M., Ames, R. and Dennis R. A. (2012). "Flow and Heat Transfer in a Jet-Impingment Configuration with no Cross-flow about Impinging Jets". Proc. ASME Turbo Expo, GT-70080.

Metzger D. E. and Korstad R. J. (1970). 'Effects of Cross-flow on Impingement Heat Transfer', ASME J. Eng. Power, p. 73-82.

Sharif M. A. R. and Mothe K. K. (2010). "Parametric Study of Turbulent Slot-Jet Impingement Heat transfer from Concave Cylindrical Surfaces," *Int. J. Thermal Sciences. Elsevier,* vol. 49, pp. 428-442.

Taslim M. E. and Rosso N. (2012). "Experimental/Numerical Study of Multiple Rows of Confined Jet IMpingement Normal to a Surface at Close Distances". Proc. ASME Turbo Expo.

Wang X., Liu R., Bai X., and Yao J. (2011). "Numerical Study on Flow and Heat Transfer Characteristics of Jet Impingement," *Proc. ASME Turbo Expo.,* GT - 45287, pp.1-10.

ISSN: 1597 – 9928. Science and Education Development Inst., Nigeria